

# Measuring the distortion of time with relativistic effects in large-scale structure

Daniel Sobral Blanco and Camille Bonvin

*Département de Physique Théorique and Center for Astroparticle Physics,  
Université de Genève, Quai E. Ansermet 24, CH-1211 Genève 4, Switzerland*

(Dated: May 6, 2022)

To test the theory of gravity one needs to test, on one hand, how space and time are distorted by matter and, on the other hand, how matter moves in a distorted space-time. Current observations provide tight constraints on the motion of matter, through the so-called redshift-space distortions, but they only provide a measurement of the sum of the spatial and temporal distortions, via gravitational lensing. In this Letter, we develop a method to measure the time distortion on its own. We show that the coming generation of galaxy surveys, like the Square Kilometer Array, will allow us to measure the distortion of time with an accuracy of 10-30%. Such a measurement will be essential to test deviations from General Relativity in a fully model-independent way. In particular, it can be used to compare the spatial and temporal distortions of space-time, that are predicted to be the same in  $\Lambda$ CDM but generically differ in modified theories of gravity.

## INTRODUCTION

Since the observation, in 1998, that the expansion of our Universe is accelerating, a variety of theories have been proposed to explain this behaviour, see e.g. [1, 2] for a review. At the level of the background, these theories are largely indistinguishable and can all reproduce the expansion rate of a cosmological constant. To discriminate between them, it is therefore necessary to look at their impact on the growth of structure. Different theories of gravity or different models of dark energy are indeed leading to a different gravitational evolution of the matter inhomogeneities. In addition, these different theories are impacting the geometry of the Universe in different ways.

The large-scale structure of the Universe offers an ideal laboratory to test these theories. On one hand, redshift surveys provide measurements of two key quantities: the dark matter inhomogeneities, denoted by  $\delta$ , and the peculiar velocities of dark matter halos,  $V$ . These quantities can be measured in a model-independent way, and then compared with predictions from any theory of gravity or dark energy model [3]. On the other hand, gravitational lensing provides measurement of the deflection of light, which is directly related to perturbations in the geometry of the Universe [4, 5]. More precisely, gravitational lensing allows us to measure the sum of the two gravitational potentials,  $\Phi + \Psi$ , where  $\Phi$  encodes deviation in the spatial part of the metric, and  $\Psi$  denotes the perturbations in the temporal part<sup>1</sup>. Again, the observed sum,  $\Phi + \Psi$ , can be directly compared with predictions from any theoretical model. Combining these three measurements,  $\delta$ ,  $V$  and  $\Phi + \Psi$ , has so far confirmed the validity of the standard  $\Lambda$ CDM model, and placed constraints on theories of modified gravity and dark energy [6–9]. The

coming generation of large-scale structure surveys, like DESI, Euclid, LSST and the SKA will drastically improve the measurements of  $\delta$ ,  $V$  and  $\Phi + \Psi$ , with the goal of unveiling deviations from  $\Lambda$ CDM and from General Relativity (GR) [10–13].

This whole framework suffers however from one important limitation: the fact that perturbations in the geometry of the Universe can only be measured via light deflection, which is sensitive to the sum of the two gravitational potentials and consequently does not allow us to measure separately  $\Phi$  and  $\Psi$ . Since modified theories of gravity generically generate differences between these two potentials, measuring them separately would provide a key test of gravity [14]. The current method consists in using Euler equation, to translate measurements of the peculiar velocity into measurements of  $\Psi$ , and then compare this with  $\Phi + \Psi$  to test for the presence or not of anisotropic stress [15]. Clearly this method fails if the theory of gravity violates Euler equation [16–21].

In this Letter, we design a method to measure  $\Psi$  directly from large-scale structure observations. We use the fact that gravitational redshift leaves an impact on the distribution of galaxies [22–24], which can be measured by looking for a dipole in the cross-correlation of bright and faint galaxies [25–32]. Gravitational redshift is an effect predicted by Einstein [33], which postulates that time passes at a slower rate in a gravitational potential well. This effect is directly sensitive to the temporal gravitational potential  $\Psi$ . It has been measured in a variety of systems: around earth, by comparing clocks at different distances from the ground [34, 35] (i.e. at different values of  $\Psi$ ); in white dwarf, by looking at the reddening of light due to its escape from the gravitational field of the star [36, 37]; and in clusters of galaxies and non-linear structures by looking at the difference in redshift between galaxies at the centre of the structure and galaxies away from the centre [38–40]. So far, all these measurements have confirmed the validity of GR. However, this effect (and consequently the potential  $\Psi$ )

<sup>1</sup> We use the perturbed Friedmann metric:  $ds^2 = a^2[-(1 + 2\Psi)d\tau^2 + (1 - 2\Phi)dx^2]$ , where  $\tau$  denotes conformal time.

has never been measured at cosmological scales, where deviations from GR may become apparent. The goal of this paper is to forecast the precision with which the potential  $\Psi$  will be measured at cosmological scales with the coming generation of surveys.

We build on a method presented in [41], where we showed that by combining different multipoles of the galaxy power spectrum, one can isolate the correlation of  $\Psi$  with the density. For our forecasts we work with the correlation function, instead of the power spectrum, since the correlation function can account for wide-angle effects, that contaminate the measurement of  $\Psi$  and need to be properly removed in order not to bias the measurement. We show that a survey like SKA will be able to measure the evolution of  $\Psi$  with a precision of 10-30 percent.

## EVOLUTION OF THE GRAVITATIONAL POTENTIAL

We start by parameterizing the evolution of the gravitational potential in a model-independent way. We assume that at early time, well in the matter era, the Universe is well described by GR. This has been tested with great precision by CMB measurements. We link therefore deviations from GR to the onset of the accelerated expansion of the Universe. In this context, the matter density perturbations in Fourier space are usually modelled as

$$\delta(\mathbf{k}, z) = T_\delta(k, z)\Psi_{\text{in}}(\mathbf{k}), \quad (1)$$

where  $\Psi_{\text{in}}$  is the primordial gravitational potential generated by inflation and  $T_\delta(k, z)$  is the density transfer function, which depends on the Fourier mode  $k$  and on the redshift  $z$ . Under the assumption that deviations from GR appear only at late time, we can write this transfer function as

$$T_\delta(k, z) = \frac{D_1(k, z)}{D_1(z_*)} T_\delta(k, z_*), \quad (2)$$

where  $T_\delta(k, z_*)$  is the transfer function predicted by GR at redshift  $z_*$ , well in the matter era. The growth function  $D_1(k, z)$  describes the growth of structure at late time and depends consequently on the theory of gravity and on the model of dark energy. At  $z_*$ , where GR is recovered, this function is independent on  $k$ .

The velocity transfer function defined through  $V(\mathbf{k}, z) = T_V(k, z)\Psi_{\text{in}}(\mathbf{k})$  is usually related to the density transfer function using the continuity equation for matter:

$$T_V(k, z) = -\frac{\mathcal{H}}{k} f(k, z) T_\delta(k, z), \quad (3)$$

where  $\mathcal{H}$  denotes the Hubble parameter in conformal time and the growth rate  $f$  is defined as

$$f(k, z) \equiv \frac{d \ln D_1(k, a)}{d \ln a}. \quad (4)$$

Under this assumption, the velocity transfer function evolves at late time as

$$T_V(k, z) = \frac{\mathcal{H}(z)f(k, z)D_1(k, z)}{\mathcal{H}(z_*)f(z_*)D_1(z_*)} T_V(k, z_*). \quad (5)$$

If the continuity equation is not valid, this standard parameterization breaks down. This would happen for example if dark matter exchanges energy with dark energy [42]. Since we want here to be agnostic about the theory of gravity, we parameterize instead the growth of velocity at late time with a new function  $G(k, z)$  such that

$$T_V(k, z) = \frac{\mathcal{H}(z)G(k, z)}{\mathcal{H}(z_*)f(z_*)D_1(z_*)} T_V(k, z_*). \quad (6)$$

Finally, the potential transfer function defined through  $\Psi(\mathbf{k}, z) = T_\Psi(k, z)\Psi_{\text{in}}(\mathbf{k})$  can be related to the density transfer function, using the Poisson equation and assuming that there is no anisotropic stress via

$$T_\Psi(k, z) = -\frac{3}{2}\Omega_m(z) \left(\frac{\mathcal{H}(z)}{k}\right)^2 T_\delta(k, z). \quad (7)$$

Under these assumptions, the gravitational potential at late time evolves as

$$T_\Psi(k, z) = \frac{\mathcal{H}^2(z)\Omega_m(z)D_1(k, z)}{\mathcal{H}^2(z_*)D_1(z_*)} T_\Psi(k, z_*), \quad (8)$$

where we have used that  $\Omega_m(z_*) = 1$ . Again, in order to be agnostic about the theory of gravity, we replace this standard evolution with a new free function  $I(k, z)$  which encodes the evolution of the gravitational potential  $\Psi$  at late time:

$$T_\Psi(k, z) = \frac{\mathcal{H}^2(z)I(k, z)}{\mathcal{H}^2(z_*)D_1(z_*)} T_\Psi(k, z_*). \quad (9)$$

The functions  $D_1(k, z)$  and  $G(k, z)$  have been measured via redshift-space distortions. The function  $I(k, z)$  on the other hand has never been measured at cosmological scales. The goal of this paper is to forecast the precision with which one can measure this function with the coming generation of surveys.

## CORRELATION FUNCTION

Redshift surveys map the distribution of galaxies in the sky and measure the galaxy number counts fluctuations

$$\Delta \equiv \frac{N(\mathbf{n}, z) - \bar{N}(z)}{\bar{N}(z)}, \quad (10)$$

where  $N$  is the number of galaxies per pixel detected in direction  $\mathbf{n}$  and at redshift  $z$ , and  $\bar{N}$  denotes the average number of galaxies per pixel at redshift  $z$ . In the linear regime, the dominant contributions to the observable  $\Delta$  are given by [22–24]

$$\Delta(\mathbf{n}, z) = b\delta - \frac{1}{\mathcal{H}}\partial_r(\mathbf{V} \cdot \mathbf{n}) + \frac{1}{\mathcal{H}}\partial_r\Psi + \frac{1}{\mathcal{H}}\dot{\mathbf{V}} \cdot \mathbf{n} \quad (11)$$

$$+ \left( 1 - 5s + \frac{5s - 2}{r\mathcal{H}} - \frac{\dot{\mathcal{H}}}{\mathcal{H}^2} + f^{\text{evol}} \right) \mathbf{V} \cdot \mathbf{n},$$

where  $r = r(z)$  is the comoving distance to redshift  $z$  and a dot denotes derivative with respect to conformal time. The functions  $b(z)$ ,  $s(z)$  and  $f^{\text{evol}}(z)$  are the galaxy bias, the magnification bias and the evolution bias of the population under consideration.

The two terms in the first line of Eq. (11) are the standard density and redshift-space distortions contributions. The third term is the contribution from gravitational redshift, which depends directly on  $\Psi$  and is the target of our study. The last two terms are Doppler contributions<sup>2</sup>.

Density and RSD generate a monopole, quadrupole and hexadecapole in the correlation function, which have been measured with various surveys, see e.g. [3]. The contributions from gravitational redshift and Doppler effects on these multipoles are strongly subdominant and can safely be neglected [43]. However, these relativistic effects generate a dipole in the correlation function, which can be measured by correlating two populations of galaxies, for example bright and faint galaxies [25]. We now write the multipoles in terms of the free functions  $D_1$ ,  $G$  and  $I$ . The even multipoles take the form

$$\xi_0(z, d) = \left[ \hat{b}^2(z) + \frac{2}{3}\hat{b}(z)\hat{G}(z) + \frac{1}{5}\hat{G}^2(z) \right] \mu_0(z_*, d),$$

$$\xi_2(z, d) = - \left[ \frac{4}{3}\hat{b}(z)\hat{G}(z) + \frac{4}{7}\hat{G}^2(z) \right] \mu_2(z_*, d),$$

$$\xi_4(z, d) = \frac{8}{35}\hat{G}^2(z) \mu_4(z_*, d), \quad (12)$$

where

$$\hat{b}(z) \equiv b(z)\sigma_8(z), \quad (13)$$

$$\hat{G}(z) \equiv G(z) \frac{\sigma_8(z)}{D_1(z)} = G(z) \frac{\sigma_8(z_*)}{D_1(z_*)}, \quad (14)$$

and

$$\mu_\ell(z_*, d) = \frac{1}{2\pi^2} \int dk k^2 \frac{P_{\delta\delta}(k, z_*)}{\sigma_8^2(z_*)} j_\ell(kd). \quad (15)$$

<sup>2</sup> Note that other relativistic distortions contribute to  $\Delta$  [22–24], but their impact on the multipoles of the correlation function is negligible [43]. Gravitational lensing also contributes to  $\Delta$ , but its impact becomes important only at large redshifts [43, 44], where we will see that  $I$  cannot be measured anymore.

The functions  $\mu_\ell(z_*, d)$  depend on the matter power spectrum at  $z = z_*$ , well in the matter era, and are therefore determined by physics in the early Universe, which is tightly constrained by CMB observations [9]. These functions are therefore considered as fixed. Measuring the even multipoles provides consequently direct measurements of the bias,  $\hat{b}(z)$ , and of the function  $\hat{G}(z)$  (which reduces to  $f(z)\sigma_8(z)$  under the assumption that the continuity equation is valid) [3].

The dipole in the cross-correlation of bright and faint galaxies reads<sup>3</sup>

$$\xi_1(z, d) = \frac{\mathcal{H}}{\mathcal{H}_0} \left\{ 3 \left( \frac{1}{r\mathcal{H}} - 1 \right) (s_B(z) - s_F(z)) \hat{G}^2(z) \right.$$

$$+ 5 \left( \frac{1}{r\mathcal{H}} - 1 \right) \left( \hat{b}_F(z)s_B(z) - \hat{b}_B(z)s_F(z) \right) \hat{G}(z)$$

$$+ \left( \hat{b}_B(z) - \hat{b}_F(z) \right) \left[ \left( \frac{2}{r\mathcal{H}} - 1 \right) \hat{G}(z) + \frac{\dot{\hat{G}}(z)}{\mathcal{H}} \right]$$

$$\left. + \frac{3}{2} \left( \hat{b}_B(z) - \hat{b}_F(z) \right) \hat{I}(z) \right\} \nu_1(z_*, d), \quad (16)$$

where

$$\hat{I}(z) \equiv I(z) \frac{\sigma_8(z)}{D_1(z)} = I(z) \frac{\sigma_8(z_*)}{D_1(z_*)}, \quad (17)$$

and

$$\nu_1(z_*, d) = \frac{\mathcal{H}_0}{2\pi^2} \int dk k \frac{P_{\delta\delta}(k, z_*)}{\sigma_8^2(z_*)} j_\ell(kd). \quad (18)$$

As before, the function  $\nu_1(z_*, d)$  which depends on  $z_*$  is considered fixed. Combining the dipole with the even multipoles provide therefore a way of measuring directly the function  $\hat{I}(z)$ , which encodes the evolution of the gravitational potential  $\Psi$ .

Note that in our derivation we have assumed that the  $k$ -dependence of  $D_1$ ,  $G$  and  $I$  is negligible, so that we can take them out of the integrals in Eqs. (15) and (18). This is a common assumption, that is used in many analyses, see e.g. [3], and that is motivated by the fact that in the quasi-static approximation the  $k$ -dependence can often be neglected [19]. However, for some theories of gravity this assumption may not be valid [47]. Relaxing it would slightly complicate the forecasts, but would not invalidate our method.

## FORECASTS

We now forecast how well we can measure  $\hat{I}$  with a survey like SKA phase 2, using the Fisher formalism. SKA2

<sup>3</sup> Note that the dipole is also affected by wide-angle effects, which generate a contribution of the form  $-2/5(\hat{b}_B - \hat{b}_F)\hat{G}d/r\mu_2(z_*, d)$ . This contribution can however be removed by constructing an appropriate estimator, as has been shown in [25, 45, 46].

TABLE I.  $1\sigma$  constraints on  $\hat{I}$  and  $\hat{G}$  relative to their corresponding fiducial value, marginalised over the bias parameters. We show the results for two values of the minimal separation  $d_{\min}$ , in Mpc/h.

	$z$	0.35	0.45	0.55	0.65	0.75	0.85	0.95	1.05
$d_{\min}$ 20	$\hat{I}$	0.225	0.243	0.277	0.326	0.392	0.481	0.601	0.767
	$\hat{G}$	0.002	0.002	0.003	0.003	0.003	0.004	0.004	0.005
$d_{\min}$ 32	$\hat{I}$	0.266	0.282	0.319	0.373	0.449	0.550	0.687	0.874
	$\hat{G}$	0.004	0.004	0.005	0.006	0.006	0.007	0.008	0.009

will observe close to a billion galaxies from  $z = 0.1$  to  $z = 2$ . We use the specifications of [10], for the number density and volume, and the fiducial cosmology is fixed to the latest *Planck* values [9]. We choose  $z_* = 10$ , well in the matter era. We split the galaxies into a bright and faint population with same number of galaxies per redshift bin. We model the bias for each of the population as  $b_B = c_B \exp(d_B z) + \Delta b/2$  and  $b_F = c_F \exp(d_F z) - \Delta b/2$  involving four free parameters with fiducial values  $c_B = c_F = 0.554$  and  $d_B = d_F = 0.783$  [10]. We assume a bias difference  $\Delta b = 1$  between the two populations, similar to what has been measured for BOSS in [29]. For the magnification bias, we use the model developed in [48], and we assume that the evolution bias vanishes for the two populations. Once data will be available the magnification bias and the evolution bias of the two populations will be directly measurable. We include shot noise and cosmic variance in the variance of the multipoles (see Appendix C of [46]) and account for cross-correlations between different multipoles.

We perform two different forecasts: the first one where we consider as free parameters the functions  $\hat{G}$  and  $\hat{I}$  in each redshift bin, and a second one where we parameterize the evolution of these functions with redshift.

### Constraints per redshift bin

From Eq. (16), we see that the dipole depends not only on  $\hat{G}$  in each redshift bin, but also on the time derivative of  $\hat{G}$ . Since we do not want to assume any evolution for  $\hat{G}$ , we express this time derivative in terms of  $\hat{G}$  in the neighbouring bins. We use the five-point stencil method:

$$\dot{\hat{G}}(z_i) = -(1+z_i)\mathcal{H}(z_i)\frac{d\hat{G}(z_i)}{dz_i} = -\frac{(1+z_i)\mathcal{H}(z_i)}{12\Delta z} \times \left[ -G(z_{i+2}) + 8G(z_{i+1}) - 8G(z_{i-1}) + G(z_{i-2}) \right] \quad (19)$$

We have checked that for redshift bins of size  $\Delta z = 0.1$ , the five-point stencil method allows us to reconstruct  $\dot{\hat{G}}(z_i)$  with a precision of 0.1 percent. On the other hand, if we use only two bins to reconstruct the time derivative we would make an error of up to 129 percent at low red-

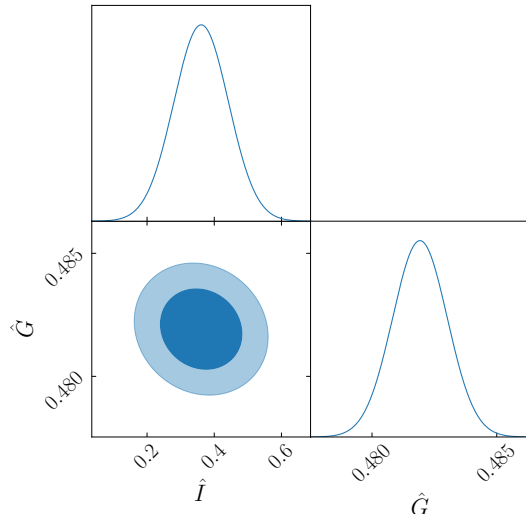


FIG. 1. Joint constraints of  $\hat{I}$  and  $\hat{G}$  at  $z = 0.35$ , with  $d_{\min} = 20$  Mpc/h.

shift, due to the fact that  $\dot{\hat{G}}$  changes sign. Such a large mistake in  $\dot{\hat{G}}$  may bias the measurement of  $\hat{I}$ .

In Table I, we show the  $1\sigma$  constraints on  $\hat{I}$  and  $\hat{G}$ , marginalised over the bias parameters. Note that due to the five-point stencil method we cannot constrain  $\hat{I}$  in the first two and in the last two redshift bins, since in these four bins  $\dot{\hat{G}}$  is not constrained. We show therefore the constraints starting at  $z = 0.35$ . We compute the constraints starting at two different minimum separations:  $d_{\min} = 20$  Mpc/h and  $d_{\min} = 32$  Mpc/h, since non-linearities have been shown to become relevant around those scales [49]. The maximum separation is  $d_{\max} = 160$  Mpc/h.

We see that at low redshift, the constraints on  $\hat{I}$  are very good, providing a direct measurement on the evolution of the potential  $\Psi$  with a precision of 20-30 percent. Since  $\Psi$  has never been measured before at cosmological scale, such a measurement will open a completely new window to test gravity. Comparing with current tests of gravity, we see that the precision with which  $\Psi$  will be measured with the coming generation of survey is similar to the precision with which the evolution of the velocity field is currently measured: in [3], for example, the combination  $f(z)\sigma_8(z)$  is measured with a precision of 10-30 percent in various redshift bins. The future constraints on  $\hat{G}$  are tighter than those on  $\hat{I}$  by almost two orders of magnitude. This is not surprising since  $\hat{G}$  is constrained by the even multipoles, which will be measured with exquisite accuracy with SKA2, whereas  $\hat{I}$  is constrained only by the dipole, which has a significantly lower signal-to-noise ratio. Interestingly, the constraints on  $\hat{I}$  are only mildly degraded (by 14 – 18%) when increasing  $d_{\min}$  from 20 to 32 Mpc/h. In contrast, the con-

TABLE II.  $1\sigma$  constraints on  $\hat{I}_0$  and  $\hat{G}_0$ , marginalised over the bias parameters, for the two models described after Eq. (21).

$d_{\min}[\text{Mpc}/h]$	No evolution		Evolution	
	20	32	20	32
$\hat{I}_0$	0.095	0.111	0.148	0.175
$\hat{G}_0$	0.001	0.002	0.002	0.003

straints on  $\hat{G}$  are degraded by 100%. This is due to the fact that the gravitational potential is much less affected by non-linearities than density and RSD.

In Fig. 1 we show the joint constraints on  $\hat{G}$  and  $\hat{I}$  at  $z = 0.35$ . We see that the parameters are almost not degenerated. This is due to the fact that the even multipoles are only sensitive to  $\hat{G}$  and can therefore efficiently break the degeneracy between  $\hat{G}$  and  $\hat{I}$  in the dipole.

Finally, we have also performed forecasts for the parameter  $\tilde{I} \equiv (\hat{b}_B - \hat{b}_F)\hat{I}$  which directly enters into the dipole. The constraints on this parameter are only very slightly better than those on  $\hat{I}$  (by 0.1 percent). Hence even though  $\hat{I}$  is completely degenerated with the biases in the dipole, these biases are so well constrained by the even multipoles, that the degeneracy is completely broken.

### Constraints from a specific time evolution

When constraining deviations from GR, standard RSD analyses usually assume a specific time evolution for the functions encoding these deviations. One common assumption is to use that the deviations evolve proportionally to the amount of dark energy  $\Omega_\Lambda(z)$ , see e.g [13]. Here we consider to the two following models for the evolution of  $\hat{G}$  and  $\hat{I}$ :

$$\hat{G}(z) = f(z)\sigma_8(z) \left[ 1 + \hat{G}_0 X(z) \right], \quad (20)$$

$$\hat{I}(z) = \Omega_m(z)\sigma_8(z) \left[ 1 + \hat{I}_0 X(z) \right], \quad (21)$$

with  $X(z) = 1$  for  $z \in [0, 2]$  in the first model and  $X(z) = \Omega_\Lambda(z)/\Omega_\Lambda(z=0)$  in the second model. With this, the analysis is significantly simplified since  $\hat{G}$  is directly determined by Eq. (20).

The marginalised constraints on  $\hat{G}_0$  and  $\hat{I}_0$  are shown in Table II. For the constant model, we reach a precision of 10% on  $\hat{I}_0$ , which decreases to 15% for the dynamical model.

### CONCLUSION

In this Letter we have shown that the coming generation of galaxy surveys, like SKA2, will be able to measure directly the evolution of the gravitational potential,  $\Psi$ , with an accuracy of 10-30%. Such a measurement will be

a game changer to test modified theories of gravity, since it is fully complementary to current measurements that are sensitive to the matter density and velocity, and to the sum of the two gravitational potentials.

One difficulty in measuring the evolution of  $\Psi$  is that it is degenerated with the time derivative of the velocity, which is itself unknown. However, we have shown that since future surveys will be able to measure the velocity in thin redshift bins, this can be used to reconstruct, in a model-independent way, the time derivative of the velocity and consequently break the degeneracy with  $\Psi$ .

Comparing our forecasts with current constraints on modified gravity, we see that future constraints on  $\Psi$  are roughly of the same order of magnitude as current constraints on the velocity  $V$ , and worse by two orders of magnitude than future constraints on  $V$ . This is simply due to the fact that the dipole (which is constraining  $\Psi$ ) has a signal-to-noise ratio which is significantly lower than that of the even multipoles (which are constraining  $V$ ). However, it is worth mentioning that the very tight constraints expected on  $V$  do not directly translate into tight constraints on modified gravity parameters, like for example  $\mu_0$  (which encodes a modification to Poisson equation) [50]. As shown in [48], if one does not assume that dark matter obeys the weak equivalence principle,  $\mu_0$  can only be constrained with a precision of 15% with a survey like SKA2, which is very similar to the constraints we found here on  $\Psi$ . This seems therefore to be the level at which modifications to GR can be tested in a truly model-independent way.

A first application of this novel measurement of  $\Psi$ , will be to use it in combination with gravitational lensing to measure the anisotropic stress in a model-independent way.

*Acknowledgements.* This project has received funding from the Swiss National Science Foundation and from the European Research Council (ERC) under the European Union’s Horizon 2020 research and innovation program (Grant agreement No. 863929; project title “Testing the law of gravity with novel large-scale structure observables”). We acknowledge the use of the `fftlog-python` code written by Goran Jelic-Cizmek and available at <https://github.com/JCGoran/fftlog-python>.

- 
- [1] K. Koyama, Rept. Prog. Phys. **79**, 046902 (2016), arXiv:1504.04623 [astro-ph.CO].
  - [2] A. Joyce, L. Lombriser, and F. Schmidt, Ann. Rev. Nucl. Part. Sci. **66**, 95 (2016), arXiv:1601.06133 [astro-ph.CO].
  - [3] S. Alam *et al.* (eBOSS), Phys. Rev. D **103**, 083533 (2021), arXiv:2007.08991 [astro-ph.CO].
  - [4] F. Köhlinger *et al.*, Mon. Not. Roy. Astron. Soc. **471**, 4412 (2017), arXiv:1706.02892 [astro-ph.CO].
  - [5] T. M. C. Abbott *et al.* (DES), Phys. Rev. D **105**, 023520 (2022), arXiv:2105.13549 [astro-ph.CO].

- [6] Y.-S. Song, G.-B. Zhao, D. Bacon, K. Koyama, R. C. Nichol, and L. Pogosian, *Phys. Rev. D* **84**, 083523 (2011), arXiv:1011.2106 [astro-ph.CO].
- [7] E. van Uitert *et al.*, *Mon. Not. Roy. Astron. Soc.* **476**, 4662 (2018), arXiv:1706.05004 [astro-ph.CO].
- [8] T. M. C. Abbott *et al.* (DES), *Phys. Rev. D* **99**, 123505 (2019), arXiv:1810.02499 [astro-ph.CO].
- [9] N. Aghanim *et al.* (Planck), *Astron. Astrophys.* **641**, A6 (2020), [Erratum: *Astron. Astrophys.* 652, C4 (2021)], arXiv:1807.06209 [astro-ph.CO].
- [10] P. Bull, *Astrophys. J.* **817**, 26 (2016), arXiv:1509.07562 [astro-ph.CO].
- [11] A. Blanchard *et al.* (Euclid), *Astron. Astrophys.* **642**, A191 (2020), arXiv:1910.09273 [astro-ph.CO].
- [12] M. Ishak *et al.*, (2019), arXiv:1905.09687 [astro-ph.CO].
- [13] S. Alam *et al.*, *JCAP* **11**, 050 (2021), arXiv:2011.05771 [astro-ph.CO].
- [14] I. D. Saltas, I. Sawicki, L. Amendola, and M. Kunz, *Phys. Rev. Lett.* **113**, 191101 (2014), arXiv:1406.7139 [astro-ph.CO].
- [15] L. Amendola, S. Fogli, A. Guarnizo, M. Kunz, and A. Vollmer, *Phys. Rev. D* **89**, 063538 (2014), arXiv:1311.4765 [astro-ph.CO].
- [16] L. Hui, A. Nicolis, and C. Stubbs, *Phys. Rev. D* **80**, 104002 (2009), arXiv:0905.2966 [astro-ph.CO].
- [17] D. Wands, J. De-Santiago, and Y. Wang, *Class. Quant. Grav.* **29**, 145017 (2012), arXiv:1203.6776 [astro-ph.CO].
- [18] J. Gleyzes, D. Langlois, M. Mancarella, and F. Vernizzi, *JCAP* **1508**, 054 (2015), arXiv:1504.05481 [astro-ph.CO].
- [19] J. Gleyzes, D. Langlois, M. Mancarella, and F. Vernizzi, *JCAP* **02**, 056 (2016), arXiv:1509.02191 [astro-ph.CO].
- [20] M. Asghari, J. Beltrán Jiménez, S. Khosravi, and D. F. Mota, *JCAP* **04**, 042 (2019), arXiv:1902.05532 [astro-ph.CO].
- [21] M. Archidiacono, E. Castorina, D. Redigolo, and E. Salvioni, (2022), arXiv:2204.08484 [astro-ph.CO].
- [22] J. Yoo, A. L. Fitzpatrick, and M. Zaldarriaga, *Phys. Rev. D* **80**, 083514 (2009), arXiv:0907.0707 [astro-ph.CO].
- [23] C. Bonvin and R. Durrer, *Phys. Rev. D* **84**, 063505 (2011), arXiv:1105.5280 [astro-ph.CO].
- [24] A. Challinor and A. Lewis, *Phys. Rev. D* **84**, 043516 (2011), arXiv:1105.5292 [astro-ph.CO].
- [25] C. Bonvin, L. Hui, and E. Gaztanaga, *Phys. Rev. D* **89**, 083535 (2014), arXiv:1309.1321 [astro-ph.CO].
- [26] J. Yoo, N. Hamaus, U. Seljak, and M. Zaldarriaga, *Phys. Rev. D* **86**, 063514 (2012), arXiv:1206.5809 [astro-ph.CO].
- [27] R. A. C. Croft, *Mon. Not. Roy. Astron. Soc.* **434**, 3008 (2013), arXiv:1304.4124 [astro-ph.CO].
- [28] C. Bonvin, *Class. Quant. Grav.* **31**, 234002 (2014), arXiv:1409.2224 [astro-ph.CO].
- [29] E. Gaztanaga, C. Bonvin, and L. Hui, *JCAP* **01**, 032 (2017), arXiv:1512.03918 [astro-ph.CO].
- [30] C. Bonvin, L. Hui, and E. Gaztanaga, *JCAP* **08**, 021 (2016), arXiv:1512.03566 [astro-ph.CO].
- [31] F. Beutler and E. Di Dio, *JCAP* **07**, 048 (2020), arXiv:2004.08014 [astro-ph.CO].
- [32] S. Saga, A. Taruya, Y. Rasera, and M.-A. Breton, *Mon. Not. Roy. Astron. Soc.* **511**, 2732 (2022), arXiv:2109.06012 [astro-ph.CO].
- [33] A. Einstein, *Annalen Phys.* **49**, 769 (1916).
- [34] R. V. Pound and J. L. Snider, *Phys. Rev.* **140**, B788 (1965).
- [35] R. F. C. Vessot, M. W. Levine, E. M. Mattison, E. L. Blomberg, T. E. Hoffman, G. U. Nystrom, B. F. Farrel, R. Decher, P. B. Eby, C. R. Baugher, J. W. Watts, D. L. Teuber, and F. D. Wills, *Phys. Rev. Lett.* **45**, 2081 (1980).
- [36] W. S. Adams, *The Observatory* **48**, 337 (1925).
- [37] J. L. Greenstein and V. Trimble, *AJ* **72**, 301 (1967).
- [38] R. Wojtak, S. H. Hansen, and J. Hjorth, *Nature* **477**, 567 (2011), arXiv:1109.6571 [astro-ph.CO].
- [39] I. Sadeh, L. L. Feng, and O. Lahav, *Phys. Rev. Lett.* **114**, 071103 (2015), arXiv:1410.5262 [astro-ph.CO].
- [40] S. Alam, H. Zhu, R. A. C. Croft, S. Ho, E. Giusarma, and D. P. Schneider, *Mon. Not. Roy. Astron. Soc.* **470**, 2822 (2017), arXiv:1709.07855 [astro-ph.CO].
- [41] D. Sobral-Blanco and C. Bonvin, *Phys. Rev. D* **104**, 063516 (2021), arXiv:2102.05086 [astro-ph.CO].
- [42] A. Pourtsidou, C. Skordis, and E. J. Copeland, *Phys. Rev. D* **88**, 083505 (2013), arXiv:1307.0458 [astro-ph.CO].
- [43] G. Jelic-Cizmek, F. Lepori, C. Bonvin, and R. Durrer, *JCAP* **04**, 055 (2021), arXiv:2004.12981 [astro-ph.CO].
- [44] F. Lepori *et al.* (Euclid), (2021), arXiv:2110.05435 [astro-ph.CO].
- [45] A. Hall and C. Bonvin, *Phys. Rev. D* **95**, 043530 (2017), arXiv:1609.09252 [astro-ph.CO].
- [46] C. Bonvin and P. Fleury, *JCAP* **05**, 061 (2018), arXiv:1803.02771 [astro-ph.CO].
- [47] T. Baker, P. G. Ferreira, C. D. Leonard, and M. Motta, *Phys. Rev. D* **90**, 124030 (2014), arXiv:1409.8284 [astro-ph.CO].
- [48] S. Castello, N. Grimm, and C. Bonvin, (2022), arXiv:2204.11507 [astro-ph.CO].
- [49] C. Bonvin, F. O. Franco, and P. Fleury, *JCAP* **08**, 004 (2020), arXiv:2004.06457 [astro-ph.CO].
- [50] L. Pogosian, A. Silvestri, K. Koyama, and G.-B. Zhao, *Phys. Rev. D* **81**, 104023 (2010), arXiv:1002.2382 [astro-ph.CO].